ELSEVIER

Thermochimica Acta 382 (2002) 65–76

thermochimica acta

www.elsevier.com/locate/tca

Accuracy in integrated circuit (IC) calorimeters

J. Lerchner[a,*], G. Wolf[a], C. Auguet[b], V. Torra[b]

[a]*Institute of Physical Chemistry, TU Bergakademie Freiberg, Leipziger Str. 29, D-09596 Freiberg/Sachsen, Freiberg, Germany*
[b]*CIRG-DFA-ETSECCPB-UPC, Campus Nord B-4, E-08034 Barcelona, Spain*

Received 29 May 2001; received in revised form 20 June 2001; accepted 22 June 2001

Abstract

As found from enthalpimetric measurements using standard test reactions systematic errors of some percent should be taken into account in integrated circuit (IC) calorimeters. The reasons of the systematic errors are analyzed by heating of sample via several Joule heaters and laser signals at different positions. The determined positional dependence of the sensitivities which is mainly caused by the planar geometry of the heat power detector can be corrected by a shape factor. © 2002 Elsevier Science B.V. All rights reserved.

Keywords: Conduction calorimeter; Chip calorimeter; Calibration constant; Sensitivity; Systematic errors; Shape factor

1. Introduction

With the design of calorimeters in the ''micro-sized'' scale appropriate conditions for the investigation of small samples are given. Recently, different constructions and applications of integrated circuit (IC) calorimeters have been described [1,2]. In general, the main part of an IC calorimeter consists of a silicon chip with integrated temperature transducer and calibration heater. As an important advantage calorimeters with very low reaction volumes (only a few microlitres) and time constants in the millisecond range result in turn with the miniaturization. In fact, a progressive miniaturization of the devices needs an increase of Seebeck effect. The Fe–constantan, the chromel–constantan, the semiconductors as the bismuth telluride and the Al–Si in the recent flat micro-sized calorimeter (Si-based) were the main steps in the last 70 years (from 1930 to 2000) [3,4]. For example, using a silicon chip with Al–Si thermopiles heat resolutions as lower as of 60 nJ can be obtained in gas–solid absorption measurements [2].

The miniaturization of conduction calorimeters to ''micro-sized'' scale progressively reduces the ratio of covered surface (RCS) by the heat flux detectors against the complete surface of the sample. This reduction of the detecting surface around the sample does not affect the repeatability of the results but does not avoid other difficulties, in particular, if accurate results will be guaranteed. In other words, the experimental system has a reduced statistical error but there are substantial differences between the used model (link between the input signal, heat power, and the output) concerning the calibration procedure and the physical reality. The differences between the assumed preconditions for the standard calibrations and the intrinsic characteristics of the actual dissipation of heat power produce the systematic error. For each geometrical, thermal and dissipation configuration

* Corresponding author. Tel.: +49-3731-392125; fax: +49-3731-393588.
E-mail addresses: johannes.lerchner@chemie.tu-freiberg.de (J. Lerchner), vtorra@fa.upc.es (V. Torra).

0040-6031/02/$ – see front matter © 2002 Elsevier Science B.V. All rights reserved.
PII: S0040-6031(01)00738-9

only an extremely reduced fraction of global dissipated heat is detected. The fraction relates to each particular configuration and the sensitivity or ''calibration constant'' is shifted with a change of configuration. The original structure (i.e. as in the older Tian–Calvet calorimeters), using a detector ''completely'' surrounding the working cell has become progressively a sensor displaying the existence of an energy dissipation process.

The progressive decrease of crucible volumes is essential to use extremely reduced masses of reagents. The mass is decreased from several grams in the Tian–Calvet calorimeters to some micrograms in the last devices. On the other hand, with the available deposition technologies the shape of the detecting system do not permit a closed surface around the crucible. The use of flat detecting surface, mainly orthogonal to the sample surface and covering an extremely reduced fraction of the global sample surface, is the origin of the relevant systematic errors. If accuracy is the expected main interest, new approach needs to be developed reducing the systematic errors. In other words, the device behavior needs to be described via more sophisticated approach of the experimental particularities.

An experimental analysis via several Joule and laser signals in comparison with heat transfer simulation establishes a way to more reliable measurements via an evaluation of the positional effects. In a first step, the positional effects can be visualized and, eventually, systematized to establish experimental rules. In a second step (out of the scope of this work) via the heat transfer equation (as Fourier equation), enhanced models explaining the sensitivity changes can be achieved.

In this work, three types of the sensitivity changes with the position of the energy dissipation are quantified. In the first one, oriented to the chemical nose effects as in gas–solid reaction and using a laser beam, the position dependence on the working surface (x–y coordinates dependence) is analyzed. The second one centers in a reacting chamber conceived for mixture analysis. Using a flat Pt resistance, the z-dependence is evaluated. In the third one, the z-dependence of the sensitivity in the case of solid samples and liquid drops which are free standing at the top of the silicon membrane of the micro-sized calorimeter is investigated by laser irradiation of the samples.

From the experimental measurements, a volume shape factor, modifying the standard Joule sensitivity determined by the manufacturer, is achieved. The shape factor includes the surface and the volume effects. Heat transfer simulations based on appropriate models show the coherence between experimental and simulated results. Calibration measurements using the protonization reaction of TRIS give some information about the validity of the derived shape factor in the case of the free standing samples (reaction in a drop deposed on the chip working surface).

2. Experimental

In our experimental investigations of the positional dependence of the sensitivity IC calorimeters based on silicon chips with integrated thermopiles were used. A chip integrated resistor (chip heater, manufacturer's Joule heater) is recommended by the manufacturer for Joule heating calibration. Detailed information of the chip and its applications are given in [1]. The chips are manufactured by XENSOR (Delft, NL) [3]. A schematic drawing of the chip is depicted in Fig. 1a. Generally, the samples are placed at the top of the silicon membrane within the area surrounded by the ''hot junctions'' of the thermocouples (Fig. 1b). In the case of flow-through devices [5], a plastic reaction chamber is attached to the chip (Fig. 1c). The chamber covers completely the available surface of the chip.

Three case studies were performed in order to analyze positional dependent sensitivity changes. In the first case, the positional dependence in x–y coordinates of the free chip is determined. Secondly, the vertical sensitivity gradient in a flow-through reaction chamber is studied. Further, in the case of free standing samples sensitivity values obtained from laser and Joule heating experiments at different vertical positions are compared.

2.1. Sensitivity dependence in x–y coordinates

Fig. 2 shows the experimental equipment used in Freiberg. Heating source is a laser diode (782 nm, Hitachi HL 7851 G) controlled by a plug-in PC interface board also equipped with ADC for data acquisition (Model Datalog DAP1200). An optical fiber serves for transmitting of the laser radiation towards

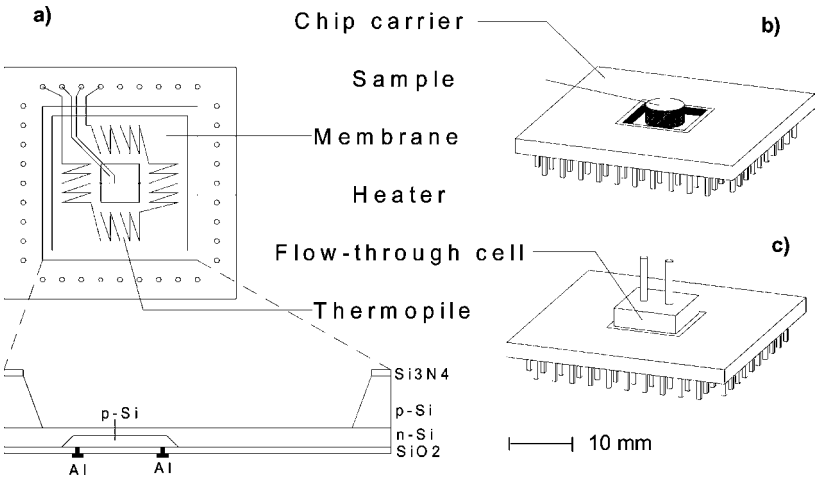

Fig. 1. Scheme of the calorimetric chip LCM 2524. (a) Structure of the chip; (b) chip with free standing sample; (c) chip with attached flow-through chamber.

a hand driven positioning table where the free end of the fiber is mounted. The free and uncovered chip is placed below the positioning table. The laser beam impinges orthogonal to the surface of the silicon membrane with an spot area close to 1 mm^2. The parasitic thermal effects induced by the reflected (highly relevant) and transmitted laser light are carefully suppressed: the external walls surrounding the measuring chamber are blackened suppressing any reentering of the reflected light in diffused form on the device and, also, a mirror reflects transmitted laser beams outward. The thermopile output is measured at different positions of the laser spot. Because of the incomplete absorption of the laser radiation only relative sensitivities can be obtained.

The laser power (∼3 mW) is modulated using a rectangular signal with a period time of 30 s. In Fig. 3a, the measured raw signal is shown (sampling: 2 ms). To increase the signal-to-noise ratio the data are averaged each 20–30 periods. The thermal response of the chip

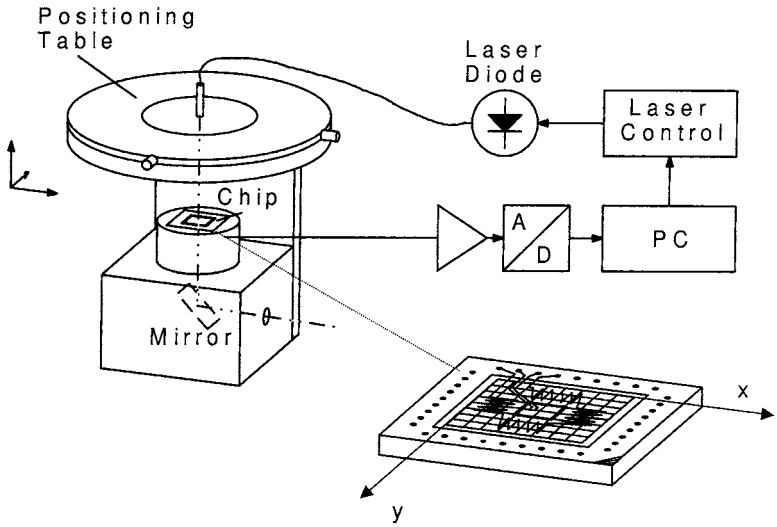

Fig. 2. Measuring system for the determination of the *x–y* sensitivity dependence of the calorimetric chip.

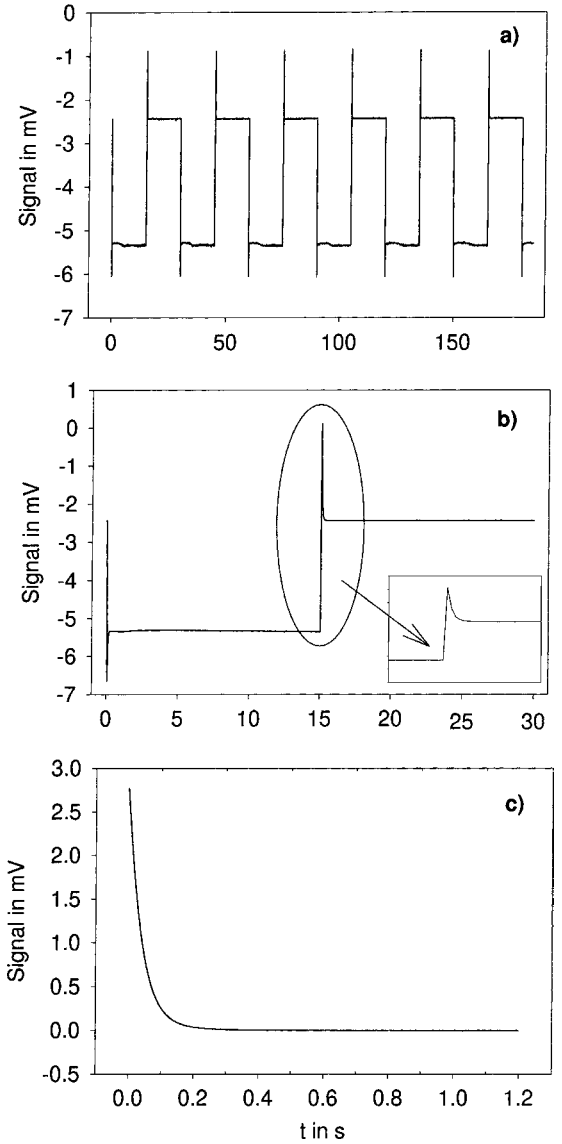

Fig. 3. Signal response of the calorimetric chip due to periodic laser irradiation. (a) Raw signal; (b) period-wise accumulated signal with zoomed part at laser switch-off edge; (c) extracted thermal decay curve.

is superimposed by photon–electron interactions. From the smoothed data (Fig. 3b), it is clearly to be seen, that a steep rise of the signal due to photon–electron interactions is followed by a slower thermal decay. The zoomed part of the graph corresponds to the falling edge of the laser pulse. At center position of the laser spot, regarding to the example in Fig. 3, the

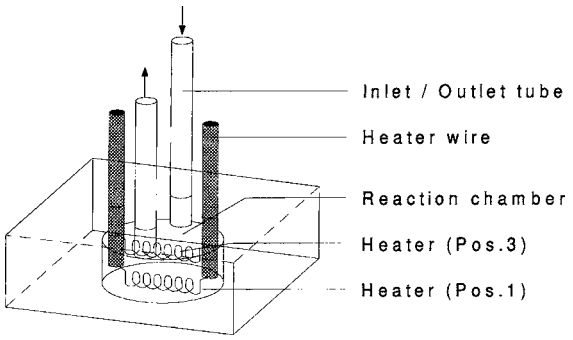

Fig. 4. Liquid flow-through calorimetric reaction chamber with auxiliary heaters at two different positions.

photon–electron interactions cause negative voltage signals. Because of the different time scales of both effects the separation of thermally induced part can be easily performed (Fig. 3c) by subtracting of the measured data 4 ms after signal rise. Preliminary measurements of *x–y*-dependence are realized using a Tektronix TDS 420 oscilloscope as digitizing instrument [6].

2.2. Determination of sensitivity gradients in a micro-sized flow-through device

To investigate vertical sensitivity variations in micro-sized flow-through devices miniaturized heaters are mounted at different positions within the reaction chamber. Diameter and depth of the reaction chamber are 4 and 1.6 mm, respectively (Fig. 4). Heaters at two of the three analyzed positions (0.25, 0.75, 1.25 mm distance from the surface of the membrane) are schematized in the figure. The chip assembly was mounted in an aluminum block to smooth the room temperature fluctuation [5]. For control of the platinum coil heaters and the chip integrated heater as well as for data acquisition the same plug-in PC interface board with ADC and DAC was used. Before starting the heating experiments the reaction chamber was filled with ethanol.

2.3. Sensitivity changes applying free standing samples

If the reactions monitored by the calorimeters take place in free standing samples the sensitivity regarding to the generated heat power should be dependent on

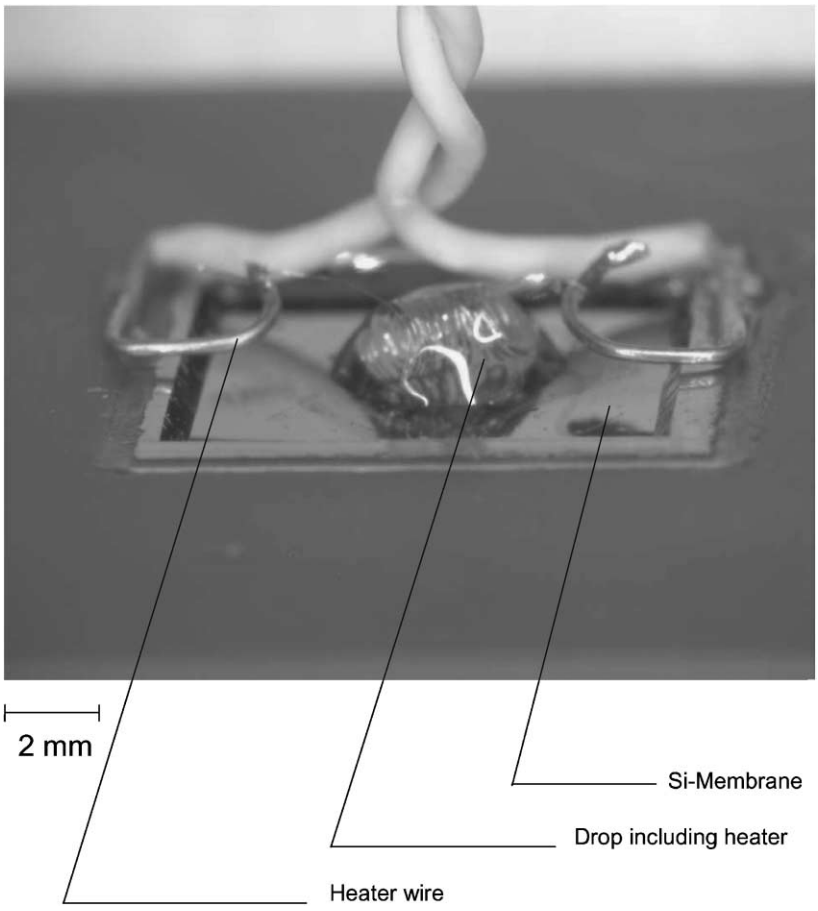

Fig. 5. Calorimetric chip with liquid drop and inserted platinum resistance heater.

the size and the thermal properties of the sample. To analyze this influence, heating measurements with Joule effect and with laser spots have been performed. For the Joule heating experiments, the chip integrated heater was used. In the other case, the blackened top surface of the samples (to ensure similar light absorption behavior on the surface) was irradiated by a laser beam in the same way as described above. The cylindrical samples (Fig. 1b) made of aluminum, graphite and polymethyl methacrylat (PMMA) are constant in diameter (4 mm) and differ in thickness (0.5, 1.0, 1.5 mm). To obtain a more realistic approach to the heat power dissipation within a free standing sample heating experiments with liquid drops of 6 μl water and glycerol ($d = 4$ mm, $h = 1$ mm), respectively, placed at the top of the silicon membrane have been performed. A platinum coil heater (platinum wire, 30 μm of diameter, resistance close to 15 Ω) situated inside into the liquid drop (Fig. 5) serves for simulation of the reaction heat power.

3. Results and discussion

3.1. Experimentally determined sensitivities

The basic time constants of the free silicon thermopile chip are in the millisecond range. Therefore, the time scales of the thermal Heaviside signals of the chip calorimeters strongly depend on the properties of the applied samples as demonstrated in Fig. 6. Laser response curves of the free, uncovered chip are shown in Fig. 6a. The different curves are related to different positions of the laser spot. The aim of Fig. 6b and c is

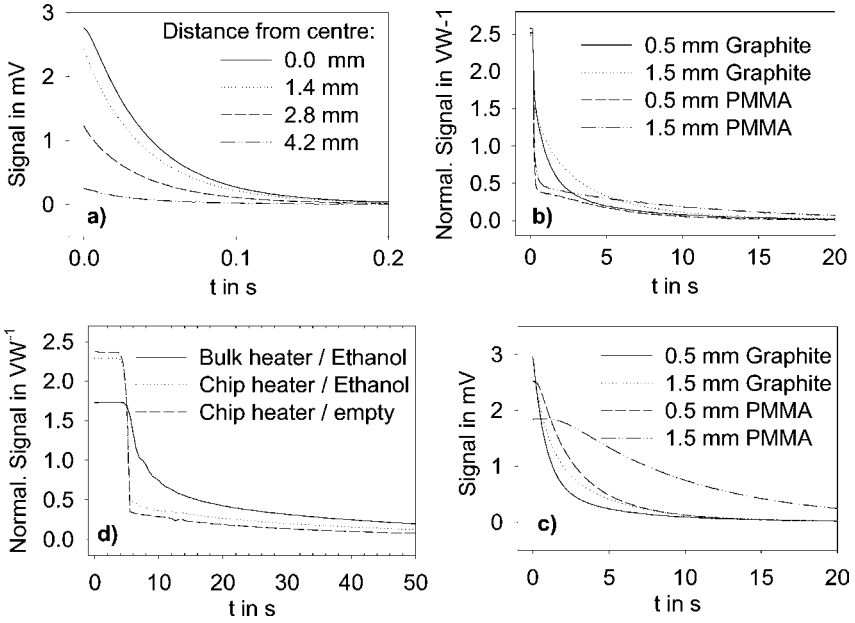

Fig. 6. Heaviside response curves of the calorimetric chip. (a) Laser spot heating at different x–y positions using a free chip; (b) Joule heating of a free standing samples using chip heater (signals divided by dissipation power): the output shows irrelevant differences at $t = 0$; (c) laser heating of free standing samples; (d) signals of the chip divided by dissipation power with attached flow-through reaction chamber.

to demonstrate the different shape of the curves dependent on whether the free standing samples are heated at the top by laser irradiation or the chip heater is used. In particular, as the signal at $t = 0$ (Fig. 6b) are similar, the exclusive use of the manufacturer's heater do not visualize the relevant changes on sensitivity related to the geometrical and thermal properties of the sample and to the dissipation position. This is one of the origins of the systematic errors in the measurements: the position of heat dissipation modifies the output signal. These effects are relatively easy to be visualized. See, for instance, in [7] a partial analysis shows the z-dependence in a classical and standard device (Differential Scanning Calorimeter 2910 MDSC, TA Instruments, 1997). The extensive plastic chamber in the case of the flow-through devices effectuates a further expansion of the time scale of the Joule heating Heaviside signals as shown in Fig. 6d.

In Fig. 7a, relative sensitivities dependent on the position in x–y coordinates obtained from steady-state signals of the laser spot measurements are shown. All data are normalized dividing by the steady-state signal measured at central position. As expected, there is a decrease of sensitivity towards the border of the silicon membrane. For comparison numerical results accomplished by using the equipment in Freiberg and Barcelona are summarized in Table 1. It can be

Table 1
Laser signal acting in the Si flat surface in free device[a]

x (mm)	y (mm)	s_r^{**} (device 660)	s_r^{**} (device 839)
1	1	0.217	0.143
2	2	0.697	0.607
3	3	0.965	1.000
4	4	1.000	1.000
5	5	0.985	0.857
6	6	0.586	0.429
7	7	0.212	0.107
1	4	0.444	0.393
2	4	0.879	0.750
3	4	0.904	0.929
5	4	0.955	0.964
6	4	0.955	0.786
7	4	0.692	0.464

[a] S_r^{**}: relative values of laser sensitivity determined from the steady-state signal at x–y coordinates divided by the steady-state signal at the center. Devices 660 and 839 were analyzed in Barcelona and Freiberg, respectively.

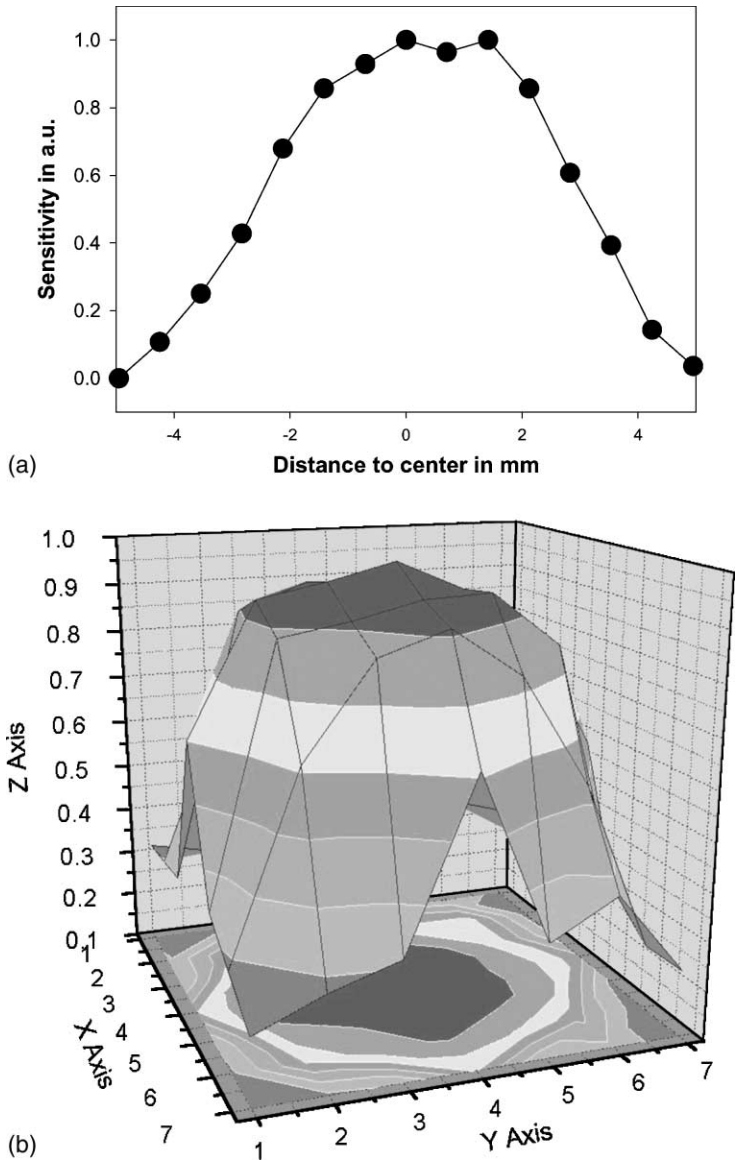

Fig. 7. Relative sensitivity dependent on the distance to center. (a) Obtained via AD converter; (b) obtained via digital oscilloscope, x–y-axis in mm, z-axis in relative sensitivity units.

deduced that the results are independent of the applied experimental method and the particular used chip. Further, if the chips show nearly the same behavior a standardization of the correction procedures seems feasible. In Fig. 7b, a more elaborated plot of the sensitivity change in x–y coordinates is represented using data measured in Barcelona.

The sensitivity investigations regarding the flow-through device give an answer in which extent systematic errors occur applying the chip heater for calibration. Fig. 8 shows the experimental results of the sensitivity against the z-axis. Point 'a' relates the Joule heating sensitivity for the chip heater. The points '1–3' are obtained from measurements using the three

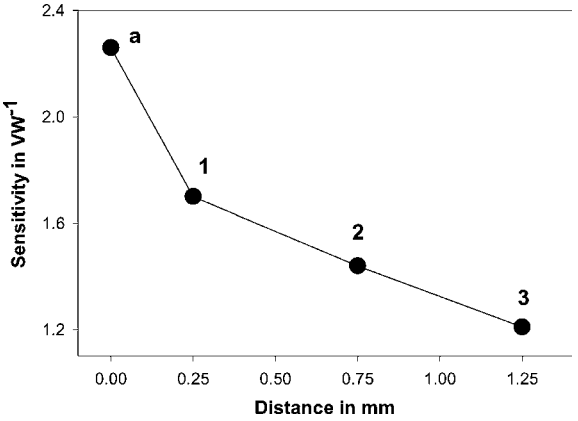

Fig. 8. Sensitivity changes with the position of heater in z-axis.

platinum wire flat resistors. The considerable near linear decrease of the sensitivity with increasing distance to the surface of the membrane should induce improvements of the design of the reaction chamber.

In most applications of IC calorimeters, the studied thermal process takes place within free standing samples placed at the top of the membrane. Also in this case (as outlined above), Joule heating applying the chip heater yields erroneous calibration results regarding the heat power evolved within the sample. In order to obtain an idea about the systematic calibration error to be expected sensitivity data achieved from Joule and laser heating experiments are compared in Fig. 9. Fig. 9a depicts that the sensitivities based on the chip heater are only poorly influenced by the sample. In contrast to the manufacturer's Joule heating (using the chip heater), the laser irradiation at the top of the sample leads to strongly size dependent sensitivity data, in particular with low thermal conductive material like PMMA. As a matter of fact, the heater is too close to the warmed junctions and cannot show the mass and thermal conductivity effects of the samples.

A more quantitative comparison between Joule and laser heating sensitivities is restricted because of the unknown part of the effectively absorbed laser radiation. Further, the thermal contact resistance induces irregularities in the size dependence of the sensitivity. Their perturbative effect is relatively increased in the case of high thermal conductive materials like aluminum and graphite (Fig. 9b).

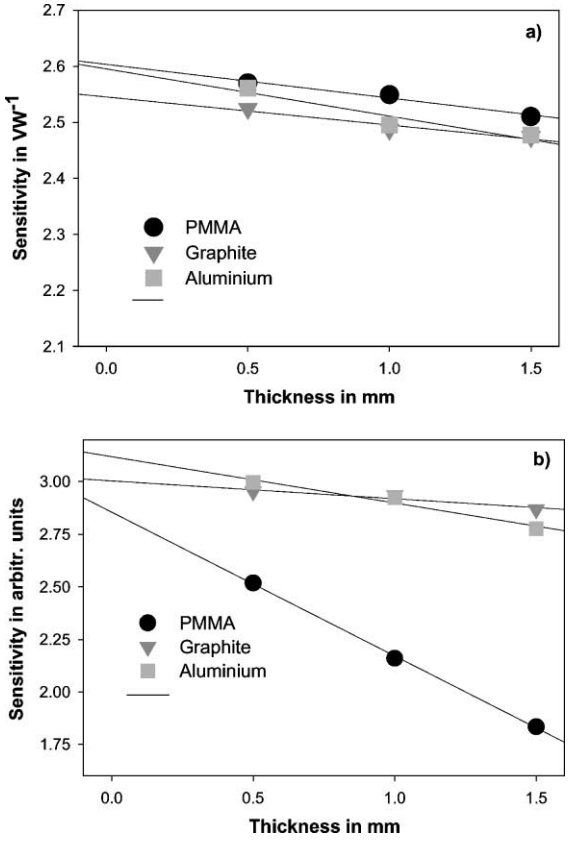

Fig. 9. Vertical positional dependent sensitivities in case of free standing samples. (a) Sensitivities determined using chip heater; (b) relative sensitivities determined by laser heating.

In the experiments, well defined but rather idealized conditions concerning real thermal processes inside the sample were established in order to obtain reliable data for modeling of the heat exchange in the calorimeter. For more realistic simulations (as the z-dependence), a miniaturized platinum heater has been inserted into a liquid drop placed at the top of the silicon membrane. In Table 2, the sensitivities of the empty and drop loaded chip are summarized. The measured data for glycerol seem to be reasonable: the chip heater sensitivity agrees well with that of the empty chip. Considering the thermal conductivity of glycerol and PMMA, 0.25 and 0.18 $W\,K^{-1}\,m^{-1}$, respectively, a decrease of 6% in the drop heater based sensitivity is in a good accordance with that of the laser heating sensitivity in the case of the 0.5 mm PMMA sample (see Fig. 9). But, it is surprising that

Table 2
Joule heating sensitivities obtained for liquid drops[a]

No.	Drop	S_{CH} (V W^{-1})	S_{DH} (V W^{-1})
1	Glycerol	2.45	2.31
2	Water	2.29	2.04
3	Water	2.26	1.81
4	Empty	2.43	–

[a] S_{CH}: sensitivity obtained with chip heater; S_{DH}: sensitivity obtained with drop inserted platinum resistance heater.

the loss of sensitivity in the case of water is higher despite of its higher thermal conductivity (0.608 W K^{-1} m^{-1}) in comparison with glycerol. One possible reason could be an increased rate of evaporation of water caused by a temperature rise during heating [8]. The much lower vapor pressure of glycerol would prevent this loss of sensitivity. On the other hand, the eventual effects of micro-convection transferring heat to the surface, i.e. increasing losses, cannot be disregarded. Between the two measurements using water (see Table 2), the drop was replaced. The difference in the drop heater sensitivity could be caused by the non reproducible shape of the drops.

A systematic error of 5–10% seems to be realistic with respect to the results of enthalpy measurements of standard reactions recently performed [9]. For example, for the protonization of Tris we found an enthalpy value of $\Delta H = -45.5$ kJ mol^{-1} (literature: 47.2 kJ mol^{-1}). In this measurements, a drop of 3 μl aqueous solution of TRIS is added to a drop of 3 μl HCl placed at the surface of the chip membrane. The measurements were performed applying drops of HCl of different concentrations. After correction of the dilution effects the molar enthalpy of protonization is obtained from the linear heat versus concentration dependency. The sensitivity was determined using the manufacturer's Joule heater.

3.2. The shape factor

Using devices with reactor chambers in 3D and detection only in a flat surface the sensitivity S depends on the positional effects. Working in the linear domain, the S value can be written as a mean of local sensitivities $S(x, y, z)$. Using the same heat power in a point resistance (Joule effect) situated in an elementary volume dV, the $S(x, y, z)$ values can be determined by the steady-state calorimetric output divided by the input heat power (a Heaviside signal). In this approach, the S value reads

$$S = \frac{1}{V}\iiint_V S(x,y,z)\,\mathrm{d}x\,\mathrm{d}y\,\mathrm{d}z \tag{1}$$

In actual measurements, as a chemical reaction, the dissipation can be considered as inhomogeneous. In this case, the mean is affected by the "weights" $w(x, y, z)$ related to the particularities in local power dissipation and the sensitivity can be written as

$$S = \frac{1}{V}\iiint_V w(x,y,z)S(x,y,z)\,\mathrm{d}x\,\mathrm{d}y\,\mathrm{d}z \tag{2}$$

The weight condition reads

$$\iiint_V w(x,\,y,\,z)\,\mathrm{d}x\,\mathrm{d}y\,\mathrm{d}z = V \tag{3}$$

For each configuration (related to the each weight distribution) a shape factor (SF) F_{xyz} can be defined from the Joule sensitivity (S_{XE}) established from the manufacturer's heater and the S value via

$$S = F_{xyz}S_{XE} \tag{4}$$

The SF "adapts" the standard sensitivity (S_{XE}) determined via Joule measurements dissipated in the resistance built by the manufacturer. Establishing the relative sensitivity S_r by

$$S_r(x,y,z) = \frac{S(x,y,z)}{S_{XE}} \tag{5}$$

The SF reads

$$F_{xyz} = \frac{1}{V}\iiint_V w(x,y,z)S_r(x,y,z)\,\mathrm{d}x\,\mathrm{d}y\,\mathrm{d}z \tag{6}$$

Obviously, the determination of $S(x, y, z)$ (or their equivalent $S_r(x, y, z)$) is, via experimental measurements, practically unavailable. In particular, an evaluation of the weight function $w(x, y, z)$ represents the knowledge of the real dissipation distribution in comparison with the calibration (Joule) procedures.

The practical target relates the assessment of some rules furnishing an approach to S. In the studied case, several different Joule analysis against z-axis and absorption of laser light can be used. In the former, using thick disks with different thermal resistance

and, in the latter, using the laser spot warming several positions in the flat surface of the free device (x–y surface at $z = 0$). Using the laser signal, the Fig. 7 shows the dependence of the sensitivity (in reduced units) against the radial position of the laser spot.

The main practical hypothesis of the SF establishes the link between S_{XE} and the ''true'' sensitivity S via a modified Eq. (4). The main hypothesis reads

- $w(x, y, z) = 1$

$$F_{xyz} = \frac{1}{V}\int\int\int_{V} S_r(x, y, z)\,dx\,dy\,dz \tag{7}$$

- Separate measurements in the silicon surface and in the z-dependence can be used. The F_{xyz} can be written as

$$F_{xyz} \approx F^*_{xy(z=0)} F_z \tag{8}$$

- The $F_{xy(z=0)}$ is evaluated using the steady-state corresponding to Heaviside laser signals

$$F^*_{xy(z=0)} = \frac{1}{A}\int\int_{A} S^*_r(x,\ y,\ z = 0)\,dx\,dy \tag{9}$$

and the $S^*_r(x,\ y,\ z = 0)$ is roughly defined by

$$S^*_r(x,\ y,\ z = 0) = \frac{S^{la}_H(x,\ y,\ z = 0)}{S^{la}_{H(XE)}} \tag{10}$$

In the previous expression (la = laser, H = Heaviside), $S^{la}_H(x, y, z = 0)$ represents the calorimetric output signal in an steady-state associated to a laser spot in x, y coordinates (a Heaviside signal directly on the silicon free surface). The $S^{la}_{H(XE)}$ is the mean of $S^{la}_H(x, y, z = 0)$ related to the position of the heater furnished by the manufacturer (for all $x, y \in \{XE\}$). The $\{XE\}$ represents the surface occupied by the resistance established by the manufacturer. Obviously, the shape of the resistance and the position dependence of the sensitivity highly influences the mean value of $S^{la}_{H(XE)}$, the particular values of $F^*_{xy(z=0)}$ and the approach to F_{xyz}.

- The F_z or the z-axis shape factor is the mean value of the Joule sensitivity. That is, determined via several two dimensional disk-flat resistances as in

$$F_z = \frac{1}{\Delta z}\int_0^{\Delta z} S_r(z)\,dz \tag{11}$$

and $S_r(z)$ is defined as in Eq. (4) particularized to the z-axis as

$$S_r(z) = \frac{S(z)}{S_{XE}} \tag{12}$$

From the position dependent laser spot measurements, the radial SF $F^*_{xy(z=0)}$ for the investigated calorimetric chip can be derived as a radius dependent polynomial expression whereas the integrated chip heater (standard Joule resistance, see Fig. 1) was considered as a squared thinned frame (side: 3.4 mm) with a mean radius (circle with the same surface) to be approached to 1.92 mm. For example, values of the radial SF calculated for planar samples of radius r and homogeneous heat power dissipation are shown in Table 3.

Table 3
Radial shape factor $F^*_{xy(z=0)}$ for the calorimetric chip LCM 2524 dissipating inside a radius, r[a]

r (mm)	$F^*_{xy(z=0)}$
1.5	1.04
2.0	0.99
2.5	0.93
3.0	0.86
4.0	0.66

[a] Homogenous heat power dissipation is assumed.

3.3. Modeling of the heat exchange

In order to examine the plausibility of the experimentally found results of the sensitivity with free standing samples (schematically a 3D system), we applied a RC network model [10,11] for simulation of Heaviside signals regarding different positions of heat power dissipation. The main effects related to sensitivity changes in the bi-dimensional free chip (in 2D) can be easily visualized using the general Fourier equation (in partial derivatives). See, for instance, in [12]. The configuration considered by the model consists of the chip membrane enclosed by the silicon rim, the sample and the chip heater. Further, thermal isolations between membrane and sample and between rim and ceramic carrier were taken into account. To model the system, it is decomposed into several elements represented by locally concentrated

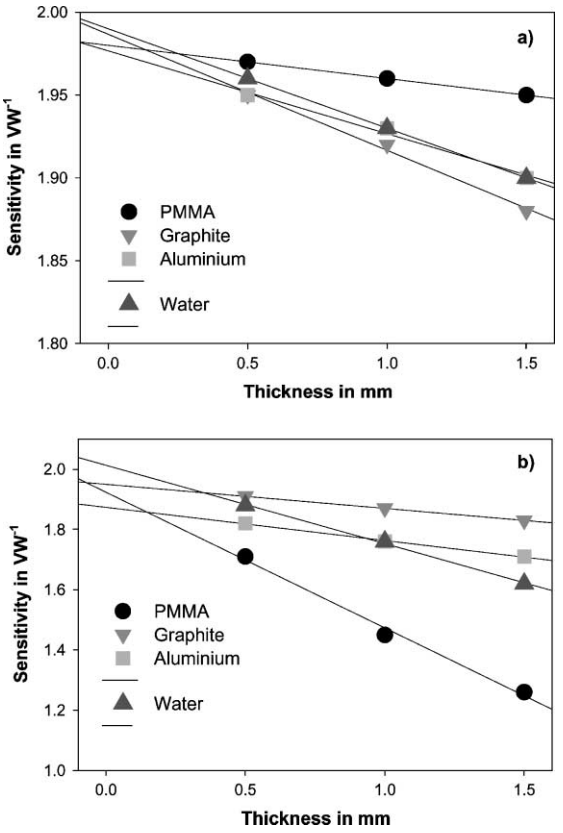

Fig. 10. Sensitivities obtained from simulated Heaviside signals. (a) simulated Joule heating; (b) simulated laser heating.

heat capacities which are interconnected by mass free thermal resistors. Further, heat transfer between all elements and the ambient air as well as that between the silicon rim and the ceramic carrier is considered. Heat capacity and thermal resistance values were calculated for the given geometry of the elements and the thermal properties of the materials. The facilities of the MATLAB software (The Math Works, Natick, USA) for the simulation of linear differential equation systems served for calculation of the Heaviside signals. Transient signals were calculated for simulated Dirac and Heaviside signals targeting the experimental step-wise Joule and laser heating at constant temperature in the surroundings. The sensitivity data were derived from the steady-state part of the simulated signals. Details of the model will be outlined in a separate paper.

In Fig. 10, the sensitivities derived from the simulated signals are shown for Joule and laser heating. The relative change with thickness of the calculated sensitivities agrees rather well with the experimental data. In addition, calculated data for water samples are introduced. A 0.5 mm thick cylindrical sample of water weighs ∼6 mg, i.e. according to the calculated data and disregarding the influence of the shape of the sample a sensitivity loss of 5–10% seems to be reasonable. From the experiments, and for each configuration, contents and considered positional dissipation, a SF and a ''mean'' sensitivity can be established diminishing the systematic error. In fact, an appropriate choice can reduce the fluctuation domain.

4. Conclusion

The miniaturization of calorimeters leads to increasing systematic uncertainties if the chip heater is the only device used for calibration. The analyzed systematic errors depend on the position of the heat power source established by the manufacturer and the experimental configuration. In the case of IC calorimeters, the errors are mainly caused by the planar structure of the heat power detector which reduces the RCS practically to zero. Systematic corrections as relevant as 40% can be needed. An increase in the reliability of the experimental results can be established via a shape factor: the SF modifies the standard Joule sensitivity determined via the manufacturer's heater and approaches to the ''true value'' for each experimental configuration.

Acknowledgements

The work is carried out in the frame of integrated actions HA 1999-0087 (MCT-Spain) and 314-Al-e-d (DAAD, Germany) between Freiberg and Barcelona group. VT acknowledges fruitful discussions on Fourier simulation analysis with Mr. F. Martorell (Barcelona).

References

[1] J. Lerchner, A. Wolf, G. Wolf, J. Thermal Anal. Cal. 57 (1999) 241.

[2] D. Caspary, M. Schröpfer, J. Lerchner, G. Wolf, Thermochim. Acta 337 (1999) 19.
[3] Liquid Nano Calorimeter, Xensor Integration, Delft, The Netherlands (website: www.xensor.nl).
[4] J.M. Köhler, E. Kessler, G. Steinhage, B. Gründig, K. Cammann, Mikrochim. Acta 120 (1995) 309.
[5] J. Lerchner, A. Wolf, A. Weber, R. Hüttl, G. Wolf, in: W. Ehrfeld (Ed.), Microreaction Technology: Industrial Prospects, Springer, New York, 2000, pp. 469–478.
[6] V. Torra, C. Auguet, H. Tachoire, P. Marinelli, J. Lerchner, J. Thermal Anal. Calorim., in press.
[7] V. Torra, H. Tachoire, Thermochim. Acta 203 (1992) 419.
[8] J.M. Köhler, G. Steinhage, J. Krause, K. Camman, Sens. Mater. 8 (1996) 357.
[9] A. Wolf, J. Lerchner, G. Wolf, in press.
[10] H. Tachoire, V. Torra, Thermochim. Acta 266 (1995) 239.
[11] V. Torra, H. Tachoire, J. Thermal Anal. 52 (1998) 663.
[12] C. Auguet, J. Lerchner, F. Martorell, F. Moll, H. Tachoire, V. Torra, Theoretical and experimental approach to nano-sized calorimetric devices, in: Proceedings of the Workshop on CIRG-ETSECCPB-UPC, 3–4 April 2001, Barcelona, C-ll-1.